JOURNAL OF GEOPHYSICAL RESEARCH, VOL. 100, NO. D11, PAGES 23,063–23,074, NOVEMBER 20, 1995

Compositional variations of sea-salt-mode aerosol particles from the North Atlantic

Mihály Pósfai[1], James R. Anderson, and Peter R. Buseck
Departments of Geology and Chemistry, Arizona State University, Tempe

Herman Sievering
Center for Environmental Sciences, University of Colorado-Denver

Abstract. Individual sea-salt-mode aerosol particles collected during the Atlantic Stratocumulus Transition Experiment/Marine Aerosol and Gas Exchange (ASTEX/MAGE) experiment in June 1992 were studied using transmission electron microscopy in both imaging and analysis modes. The set of eight samples provided an opportunity to compare "clean," "intermediate," and "dirty" oceanic aerosols. In the clean samples, major species include NaCl, mixed-cation (Na, Mg, K, and Ca) sulfates, and in some particles, $NaNO_3$. The same compounds also occur in intermediate samples, but compositional groups can be distinguished that are characterized by low- and high-Cl losses from sea salt. In these samples, most Cl loss is compensated by $NaNO_3$ formation. Several compositional groups occur in the dirty samples; these include, in addition to the particle types in clean and intermediate samples, Na_2SO_4 (with minor Mg, K, and Ca), $(NH_4)_2SO_4$, and silicates. The uniform compositions of sea-salt-mode particles in the clean samples suggest that the same process was acting on all particles. Their excess sulfate and nitrate probably formed through the oxidation of SO_2 in the sea-salt aerosol water and by reactions between NO_x and NaCl. On the other hand, distinct compositional groups in the dirty samples reveal that long-range transport of continental air masses resulted in the mixing of aerosols that were exposed to different conditions. In addition to O_3 oxidation, cloud processing may have contributed to the formation of excess sulfate in these samples.

Introduction

Sea-salt-mode oceanic aerosol particles are important in the global cycles of S, N, and Cl, thereby influencing climatic processes. A significant portion of S is removed from the atmosphere through the oxidation of SO_2 in the water associated with sea-salt particles [*Sievering et al.,* 1991, 1992; *Chameides and Stelson,* 1992]. In the marine atmosphere, N-bearing species such as HNO_3 and NO_2 are also available for reactions with sea-salt [*Huebert et al.,* 1990; *Finlayson-Pitts,* 1983]. When NaCl converts to sulfate and nitrate, Cl is released into the atmosphere.

Although these processes involving marine aerosols are now reasonably well understood, several details are not accurately known. Since SO_2 in the marine atmosphere can originate from both natural and anthropogenic sources, it is difficult to estimate the effects of continental disturbances on sea-salt conversion [*Chameides and Stelson,* 1992]. Owing to the conversion of NaCl into sulfates, rapid temporal and spatial variations occur in the compositions of remote oceanic aerosols (T. W. Shattuck et al., The background aerosol in the remote equatorial Pacific: Individual-particle analysis of samples from the FeLINE-I cruise, submitted to *Environmental Science and Technology,* 1995); however, little is known about such variations in continentally affected sea-salt-mode aerosols. For the calculation of S budgets in the remote atmosphere, it is necessary to know whether S-bearing particles are transported from the continent into the remote oceanic environment. Also, several studies have shown that Cl losses are not entirely compensated by sulfate and nitrate formation [*Keene et al.,* 1990; *Pszenny et al.,* 1993a]; the mechanism by which this additional Cl is lost is in dispute [*Keene et al.,* 1993; *Chameides and Stelson,* 1993].

We have shown that chemical species in marine aerosol particles can be identified using analytical transmission electron microscopy [*Pósfai et al.,* 1994]. In the present study we used the same method to study particles collected near the Azores Islands in the North Atlantic. Our goal is to understand the atmospheric transformation and transport of sea-salt-mode marine aerosols. We address several questions: What particle types occur in this North Atlantic aerosol? Are sulfates and nitrates uniformly distributed on every particle? Do anions other than $SO_4^{=}$ or NO_3^{-} compensate for Cl losses? What processes formed these aerosols? How do clean and polluted oceanic aerosols differ? How does the continental influence perturb natural processes?

Experiment

Aerosol samples were collected during the June 1992 Atlantic Stratocumulus Transition Experiment/Marine Aerosol and Gas Exchange (ASTEX/MAGE) experiment in the North Atlantic. Atmospheric particles were collected directly onto Cu

[1]Now at Department of Mineralogy, University of Veszprem, Veszprem, Hungary.

Paper number 95JD01636.
0148-0227/95/95JD-01636$05.00

electron microscope grids that were placed on the third stage of a Casella cascade impactor. The sampling point was on the bow tower of the research vessel *Malcolm Baldrige,* 10-m above sea level. We studied eight grid samples, two each from the first Lagrangian (IL1) and the ship-only (S1) intensives, and four samples from the second Lagrangian (IL2) intensive (Table 1). Particle loadings on the grids are ideal for transmission electron microscopy (TEM) (Figure 1); the particles are well separated, so it is unlikely that many particles aggregated on the grid. The size cut for the third stage of the impactor is 0.7 μm as specified by the manufacturer. Observed particle diameters range from ~0.4 to 6 μm, with most in the 1- to 2-μm range. Size distributions are not uniform; particles within the central area of the grid (which was under the inlet of the impactor) are larger than the peripheral ones. No contamination was detected.

The aerosol particles were studied using a JEOL 2000FX electron microscope operated at a 200-kV accelerating voltage and equipped with a double-tilt (±60°; ±45°) goniometer stage. TEM images were used to observe particle morphologies. The structures of crystalline phases were identified using selected-area electron diffraction (SAED). Particle compositions were determined by energy-dispersive X ray spectrometry (EDS), using an attached ultrathin-window KEVEX detector that allowed the detection of C and heavier elements. We analyzed standards to determine experimental Cliff-Lorimer sensitivity factors (*k* factors [*Cliff and Lorimer,* 1975]) for Na, Mg, S, Cl, K, and Ca. Extreme care was taken to avoid electron beam damage to the particles during the acquisition of EDS spectra. The X ray spectra were then processed and quantified using the thin-film routine of the Quantex software. The concentrations of elements lighter than Na were not determined quantitatively because the absorption within the specimen is very large for low-energy X rays (such as those emitted by N and O), and the overlapping peaks make intensity measurements difficult.

We relied on EDS analyses for identifying most chemical species. However, it is difficult to determine the compositions of species that contain light elements such as N and O. Independently of whether the particles crystallized on the grid or in the air, their crystal structures are related to their compositions. Therefore we used electron diffraction to identify their structures and thus confirmed the EDS identifications.

Results

Identification of Individual Components in Particles

NaCl. Crystals of NaCl are readily identified from both their SAED patterns and EDS spectra. NaCl crystals in each sample are aggregated with other species, most commonly mixed-cation sulfates (Figure 2).

Sulfates. Sulfate crystals occur both in association with other species and as individual particles. They form rod-shaped (Figure 2a) or tabular crystals (Figure 3a), or they have no distinctive morphologies (Figure 2b), i.e., they are anhedral. The major metal in sulfates is Na, but they also typically contain Mg, K, and Ca (Figure 3b). The compositions of individual crystals are variable. As pointed out by *Pósfai et al.* [1994], the striking rod-shaped morphologies are associated with an elevated Ca content. We use the term "mixed-cation sulfates" for crystals that have a (Mg+K+Ca)/Na atomic ratio higher than ~0.2, and "Na_2SO_4 (with minor Mg, K, and Ca)" for those having (Mg+K+Ca)/Na < ~0.2.

Sulfates of Na, Mg, K, and Ca can form in a variety of structures, all of which are related to that of hexagonal Na_2SO_4 (I) (Figure 3c), which is the high-temperature polymorph of Na_2SO_4. According to *Eysel et al.* [1985], this structure can be stabilized at room temperature by various substituting cations; K^+ can completely replace Na^+, and even divalent cations such as Ca^{2+} and Mg^{2+} can substitute for Na^+. Depending on the composition, several slightly distorted varieties of the Na_2SO_4 (I) structure occur [*Eysel,* 1973; *Eysel et al.,* 1985].

The aerosol sulfates apparently form structures that differ from those of common evaporite minerals. We think that the rather special environment of aerosol droplets and the ability of Na_2SO_4 (I) to accommodate variable amounts of Na^+, Mg^{2+}, K^+, and Ca^{2+} (the major cations in seawater aerosol droplets) explain why sulfates in marine aerosols crystallize in this structure or in its derivatives. In addition to the basic Na_2SO_4 (I) structure, some sulfates have superstructures of Na_2SO_4 (I), a probable result of the ordering of $SO_4^=$ groups. However, when exposed to the electron beam for several seconds, the superlattice reflections disappear and the structure transforms into the Na_2SO_4 (I) polymorph.

$NaNO_3$. $NaNO_3$ is common in our samples. In Figure 4a it is attached to NaCl and mixed-cation sulfates. The small peak

Table 1. Sample Numbers, Sampling Dates and Times, Meteorological and Black Carbon Data

	IL1		IL2				S1	
	9	11	18	19	20	25	28	29
Sampling date	June 13	June 13	June 19	June 19	June 19	June 20	June 24	June 24-25
Sampling time	0112 to 0509	0950 to 1429	0246 to 0659	0713 to 1123	1137 to 1547	0958 to 1404	1708 to 1940	2206 to 0138
Latitude, °N	30.98	31.25	31.57	31.59	31.58	31.78	28.32	28.18
Longitude, °W	26.48	26.32	26.46	26.39	26.21	21.84	23.43	23.37
Temperature, °C	19.9	19.9	20.1	20.1	20.2	19.3	18.8	13.8
True wind speed, m/s	5.1	7.1	3.6	3.9	3.2	7.1	3.4	2.2
Relative humidity, %	85	79	85	83	79	65	68	71
UV radiation, W/m^2	0.20	35.6	0.3	20.8	53.5	45.4	17.8	0.1
Black carbon, ng/m^3	43.3	7.2	266	205	77.5	152	50	68.5

IL1, first Lagrangian intensive; IL2, second Lagrangian intensive; S1, ship-only intensive.

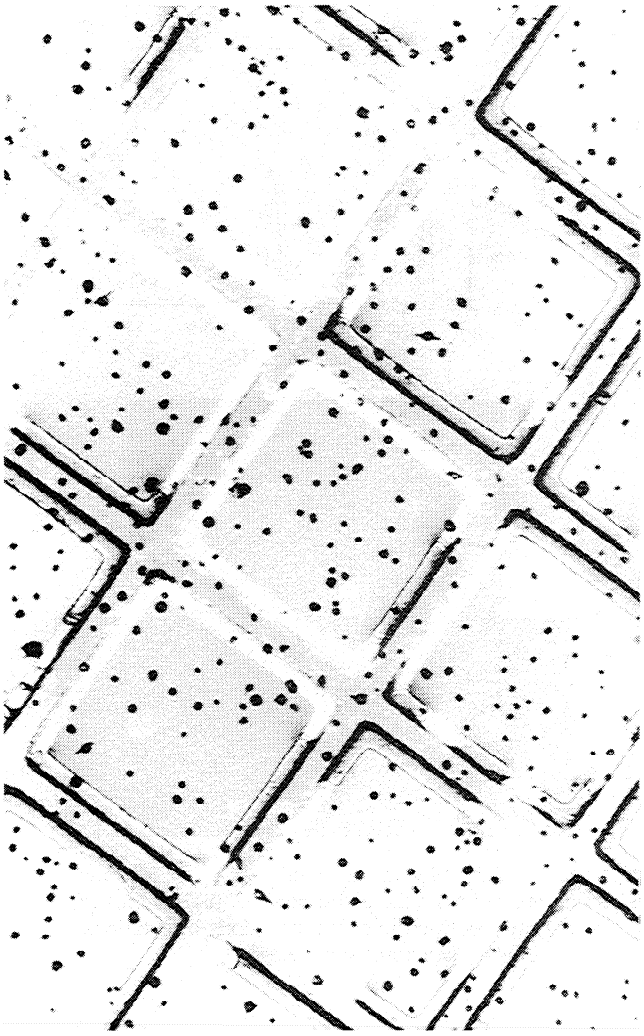

Figure 1. A portion of sample 9 as seen with an optical microscope. The edge of one mesh of the Cu TEM grid is about 100 μm long. The dark spots are the aerosol particles.

at ~0.4 kV (Figure 4b) indicates N. SAED patterns confirm that the crystal has the nitratite ($NaNO_3$) structure (Figure 4c). Pure $NaNO_3$ is the major phase in a large number of particles in some samples. The other constituent of these particles is mixed-cation sulfate (Figure 5).

$(NH_4)_2SO_4$. Supermicron $(NH_4)_2SO_4$ particles occur in several samples. Particles like the one in Figure 6a are extremely sensitive to the electron beam. A large portion of the particle is vaporized by the beam within a few seconds, and only some S-containing residue remains on the grid. Therefore EDS spectra obtained from such particles provide only limited information about their composition; they indicate the presence of S, O, and perhaps N. SAED patterns match those for the mineral mascagnite, $(NH_4)_2SO_4$.

Crustal particles. Silicates are abundant in the IL2 samples; we identified quartz, feldspar, and sheet silicates. The most common crustal particles are smectites (Figure 7), which are Mg- and Fe-bearing clay minerals with high swelling and cation-exchange capacities. A general formula for tri-octahedral smectites is $(1/2Ca,Na)_{0.7}(Mg,Fe,Al)_6[(Si,Al)_8O_{20}](OH)_4 \cdot nH_2O$ [*Deer et al.*, 1992]. The mineral particles are typically attached to NaCl, mixed-cation sulfates, and $NaNO_3$. Elongated crystals of anhydrite ($CaSO_4$) occur in some samples; their structures distinguish them from the sulfates that were described above. Anhydrite crystals are commonly associated with clay minerals (Figure 7b).

A few rounded aluminosilicates also occur in the samples (Figure 8). Such particles produce no electron diffraction patterns, and they commonly contain Fe and minor amounts of Ti, V, and P. We interpret them as fly-ash particles.

Systematic X Ray Analyses

We analyzed ~30 to 100 particles in each sample in order to characterize the compositions and distributions of chemical species for entire samples. We outlined two or three rectangular areas on a TEM grid and obtained EDS spectra from each particle within these regions (Figure 9). (The collection efficiency for particles of different Stokes numbers varies as a function of radial distance from the center of the impactor jet

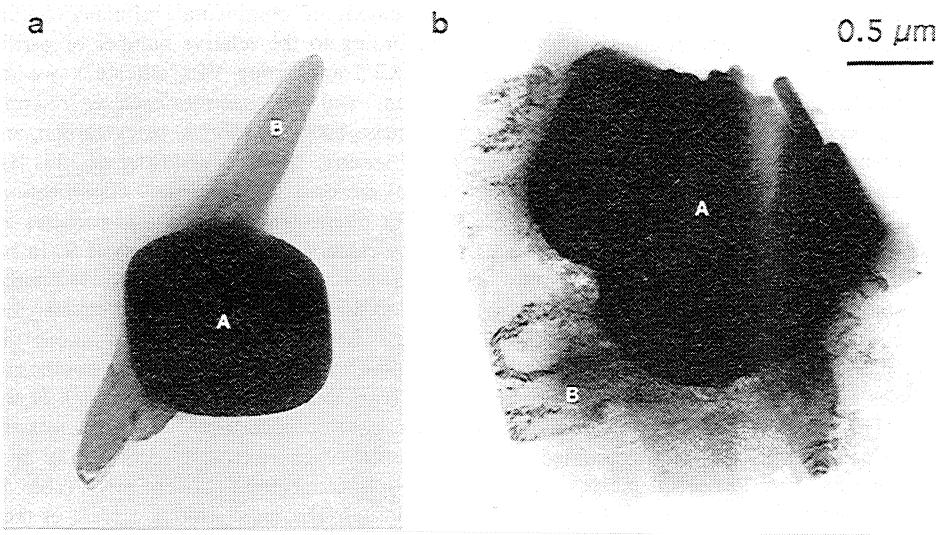

Figure 2. TEM images of particles consisting of NaCl (labeled A) and mixed-cation sulfates (labeled B). (a) is from sample 28, and (b) is from sample 29.

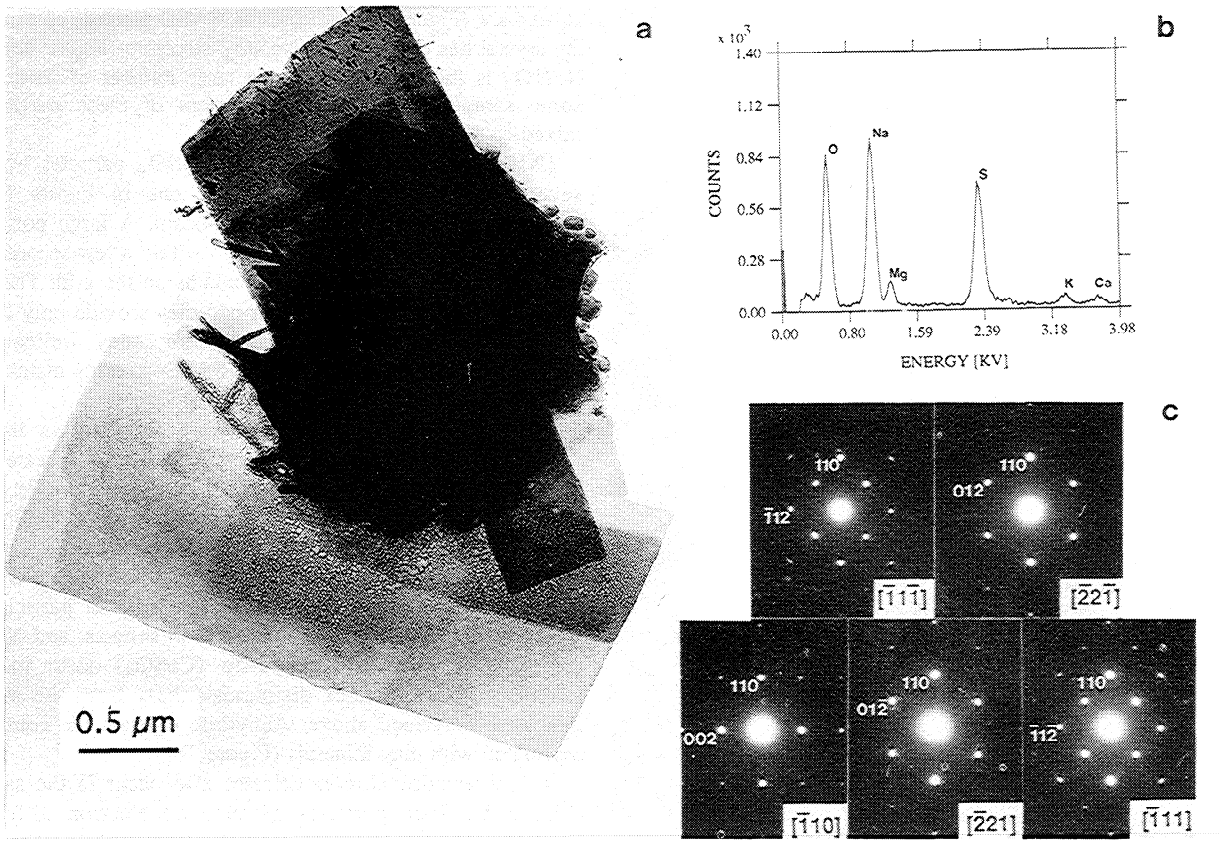

Figure 3. (a) Na_2SO_4 particle. Both the tabular crystals and the dark spot in the middle of the image are Na_2SO_4; they contain minor Mg, K, and Ca. (b) EDS spectrum obtained from the entire particle. (c) A series of SAED patterns obtained from a tabular Na_2SO_4 crystal. The crystal was tilted into five zone-axis orientations. Reciprocal lattice spacings and angles are consistent with the Na_2SO_4 (I) structure (sample 18).

[*Sethi and John,* 1993]. Therefore it is likely that particle compositions obtained from a given analysis region on the grid do not represent ambient particle concentrations. In order to minimize this potential sampling bias, two analysis regions were chosen consistently at the center and at the peripheral area of the deposition pattern in each sample; when a third region was analyzed, it was chosen at a location halfway between the center and the edge. We did not detect any changes between the compositions of particles in central and peripheral areas. It is possible that the number of analyzed particles was too small to give a systematic difference between the compositions of different size ranges.) For these analyses we spread the electron beam so that it was large enough to include whole particles with all their individual components; in this way we ensured that the resulting compositions are as close as possible to those of the original, airborne particles. In order to determine what species contribute to these "bulk" compositions, we identified the individual crystals in several dozen representative particles.

The particle analyses are plotted in relative atomic percents in Figures 10 to 12. The numbers along the horizontal axes represent the analyzed particles. Similar particle compositions were plotted next to one another. The small masses of some particles made a reasonable quantitative analysis impossible; the number of such particles is given in the captions for each sample.

Compositional groups. The results of the systematic analyses show that some samples contain particles with uniform compositions, whereas distinct compositional groups can be distinguished in others. Based on the major species, we defined six compositional groups (marked by roman numerals and given in Table 2). The group numbers are also marked in the corresponding sections of Figures 10 to 12. As discussed below, the distribution of particles over the six groups reflects the extent of continental influence on the marine aerosol. According to the relative number of particles within group I ("NaCl") and group VI ("silicate"), we termed two samples "clean," and three samples each as "intermediate" and "dirty." Air-mass back-trajectories, black carbon, and other data (Table 1) [*Pszenny,* 1993; *Sievering et al.,* this issue; *Kim et al.,* this issue] are consistent with this classification.

The diameters of all analyzed particles are larger than 1 μm in the clean samples and in sample 9. In two intermediate (20 and 28) and in two dirty (19 and 25) samples, the diameters of 10% to 30% of the particles are smaller than 1 μm. However, there is no systematic difference among the size distributions of particles belonging to distinct compositional groups.

Clean samples. Samples 11 and 29 were collected under clean oceanic conditions. Air-mass back-trajectories show no evidence of continental effects on the aerosol; black carbon and SO_2 concentrations were low (Table 1) [*Sievering et al.,* this issue]. The most striking feature of these clean samples is that particles have uniform compositions (Figures 10b and 11b). All particles in sample 11 consist of NaCl, mixed-cation (Na, Mg, K, Ca) sulfates, and an amorphous material that contains Mg, Cl, and O. Particles in sample 29 also consist of

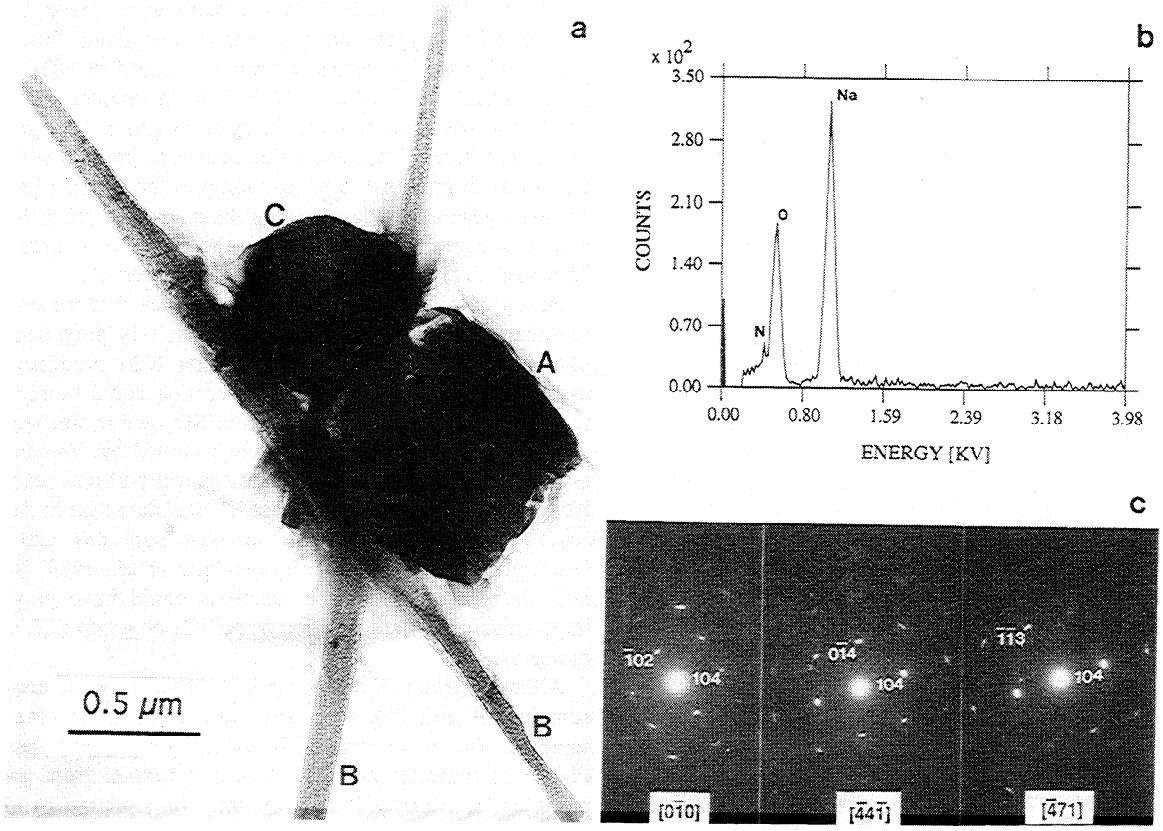

Figure 4. (a) Aerosol particle consisting of $NaNO_3$, (labeled A), mixed-cation sulfates, (labeled B), and NaCl (labeled C). (b) EDS spectrum obtained from the $NaNO_3$ crystal in Figure 4a. (c) SAED patterns obtained from another $NaNO_3$ crystal. The central diffraction pattern is identical to that obtained from the $NaNO_3$ crystal in Figure 4a (sample 20).

NaCl and mixed-cation sulfates, and $NaNO_3$ was identified in several particles.

Intermediate samples. Particles in the three intermediate samples (9, 20, and 28; Figures 10a, 12c, and 11a, respectively) belong to several compositional goups. Group I contains the largest number of particles in all three samples. These particles consist of NaCl and mixed-cation sulfates. $NaNO_3$ also occurs in some of them. Particles in group II of sample 9 and in group III of samples 20 and 28 consist mainly of $NaNO_3$. The particle shown in Figure 5 is characteristic of group III. A small number of Na_2SO_4 particles (groups IV and V) occur in samples 9 and 20, and a few silicates were observed in all three samples.

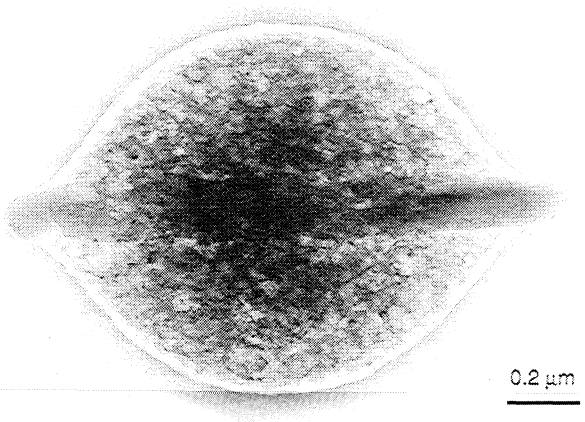

Figure 5. Aerosol particle consisting mostly of $NaNO_3$. The horizontal, rod-shaped crystal is mixed-cation sulfate (sample 20).

Dirty samples. Three samples (18, 19, and 25; Figures 12a, 12b, and 12d, respectively) that were collected during IL2 show evidence of strong continental influence. Particles containing silicate (group VI), Na_2SO_4 (group V), and individual $(NH_4)_2SO_4$ particles are common, whereas group I particles are relatively sparse. Sample 18 is the "dirtiest"; group I particles are missing, and it contains the largest relative number of group V and VI particles. Individual $NaNO_3$ particles (group III) are absent from sample 18, but are abundant in sample 25. Group VI includes particles with variable compositions; this is because the mass of crustal particles is variable, and they can be attached to any particles of groups I to V.

Discussion

Sea Salt Conversion

Atomic ratios obtained from particles in groups I to V indicate that these particles originated from seawater droplets. Ratios of major elements relative to Na are compared to seawater values in Table 3 for each group in every sample. Anions other than Cl^- and $SO_4^=$ are represented in the column labeled A^-; these values are calculated to balance the excess positive charge of the particles. In all five groups the ratios of Mg, K, and Ca to Na are close to those characteristic of

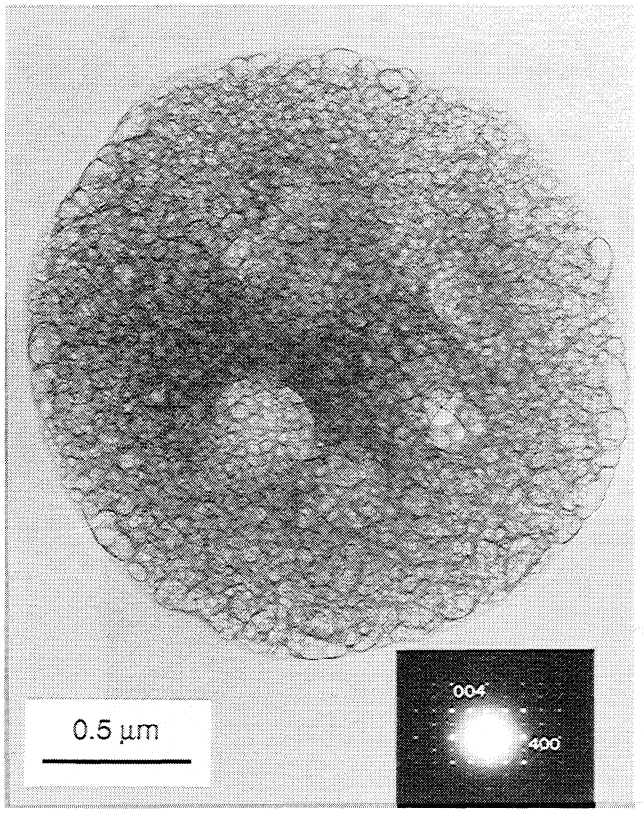

Figure 6. $(NH_4)_2SO_4$ particle (sample 18). The bubbles in the particle are caused by electron-beam damage. The SAED pattern was obtained from another, similar-looking particle in sample 19.

seawater (see the bottom row of Table 3). The anions, however, show a large variability, as is also obvious from Figures 10 to 12.

Groups I to V represent different stages of sea-salt conversion, ranging from fresh particles (group I) to practically Cl-free nitrates and sulfates (groups III, IV, and V). The amount of Cl in group I particles is between 17 and 38 at. % lower than in seawater. This Cl loss is at least partly balanced by sulfate and nitrate formation. We believe the O_3 oxidation mechanism of *Sievering et al.* [1992, this issue] is largely responsible for the formation of mixed-cation sulfate in group I particles. Most sulfate that forms through such oxidation in the sea-salt aerosol water accumulates in 200 to 1000 s [*Chameides and Stelson,* 1992]; this short reaction time may explain the relatively uniform compositions of particles within group I. (Longer reaction times would result in the sampling of particles that have a range of compositions between those of unreacted sea-salt and group I particles.) Under clean oceanic conditions the source of the SO_2 for this reaction is probably marine.

In addition to the O_3 oxidation mechanism, other processes that form sulfates and nitrates were likely active in the particles of groups II to V. Variations in the compositions of group II particles indicate its transitional character. In samples 9, 25, and 28 the S/Na ratio is about the same for group II and group I particles. However, this ratio is significantly higher in group II than in group I for samples 19 and 20. Hence the additional Cl loss in group II particles can primarily be compensated by either nitrate or sulfate.

$NaNO_3$ forms the bulk of the particles in group III. The atomic ratios suggest that particles of this group form when the Cl^- of group I particles is entirely replaced by NO_3^- (Table 3; cf. entries for Δ Cl/Na and Δ A^-/Na). In samples 19, 20, 25, and 28 the S/Na ratio is about the same for group I and group III particles, whereas the Cl/Na value decreases from ~0.8 in group I to ~0.07 in group III. The four samples that contain group III particles were all collected during the day, when photochemical reactions could occur. The only other daytime sample is the "cleanest" (11), in which no $NaNO_3$ was observed.

Based on our limited samples, it appears that the complete replacement of Cl^- by NO_3^- in sea salt is governed by a photochemical reaction, provided that NO_3^- precursors are available in the atmosphere. This reaction could be related to the daytime formation of HNO_3 from NO_2 and photochemically produced OH. Similar results were obtained by *Mamane and Gottlieb* [1992], who showed that sea-salt particles react with HNO_3 and NO_2 much faster under UV radiation than in the dark. N_2O_5 and NO_2 react with sea salt both day and night [*Finlayson-Pitts,* 1983; *Finlayson-Pitts et al.,* 1989; *Behnke and Zetzsch,* 1990]; these reactions could have played an important role in the formation of $NaNO_3$ on group I, II, and IV particles.

Although group IV and V particles occur in two intermediate samples (9 and 20), they are more abundant in the dirty samples. The S/Na and Cl/Na values for group V particles (Table 3) indicate that they probably formed from group I particles in which Cl^- was completely replaced by $SO_4^=$. Particles in group IV are intermediate in composition between groups III and V; Cl is almost completely lost and replaced by sulfate and nitrate. Reactions that could form the excess sulfate in group IV and V particles include continued oxidation of SO_2 by O_3 and by H_2O_2 [*Chameides and Stelson,* 1992], coalescence between H_2SO_4 droplets and NaCl in clouds [*Andreae et al.,* 1986], and in-cloud reactions [*Hegg et al.,* 1984]. However, *Sievering et al.* [1991] concluded that in-cloud processes could explain only about 5% of the non-sea-salt sulfate associated with sea salt under meteorological conditions (relative humidity, cloud cover, and SO_2 concentrations) similar to those that prevailed during the ASTEX/MAGE experiment.

The major anion replacing Cl^- in sample 18 is $SO_4^=$, while in sample 20 it is NO_3^-. This separation of sulfate and nitrate means that their sources, their formation mechanisms, or both are different. The distribution of group V particles over the samples parallels the distribution of crustal (group VI) particles. While the source of the excess sulfate is thus apparently continental, the origin of nitrate precursors is less obvious. There is a large number of group III particles even in the relatively clean sample 28.

The SO_2 oxidation by O_3 in the sea-salt aerosol water during ASTEX/MAGE was studied by *Sievering et al.* [this issue]. They obtained good agreement between observed and predicted sulfate concentrations, except for sample 18 (in which the observed concentration is too high) and sample 20 (in which the predicted concentration is too high). Our results show that in sample 18 there was a continental input of sulfate to the aerosol in the form of anhydrite ($CaSO_4$). The presence of $(NH_4)_2SO_4$ in sample 18 could also result in high measured sulfate concentrations that are not associated with the O_3 oxidation mechanism. On the other hand, the abundance of group III particles in sample 20 suggests that high concentrations of HNO_3 reduced the efficiency of SO_2

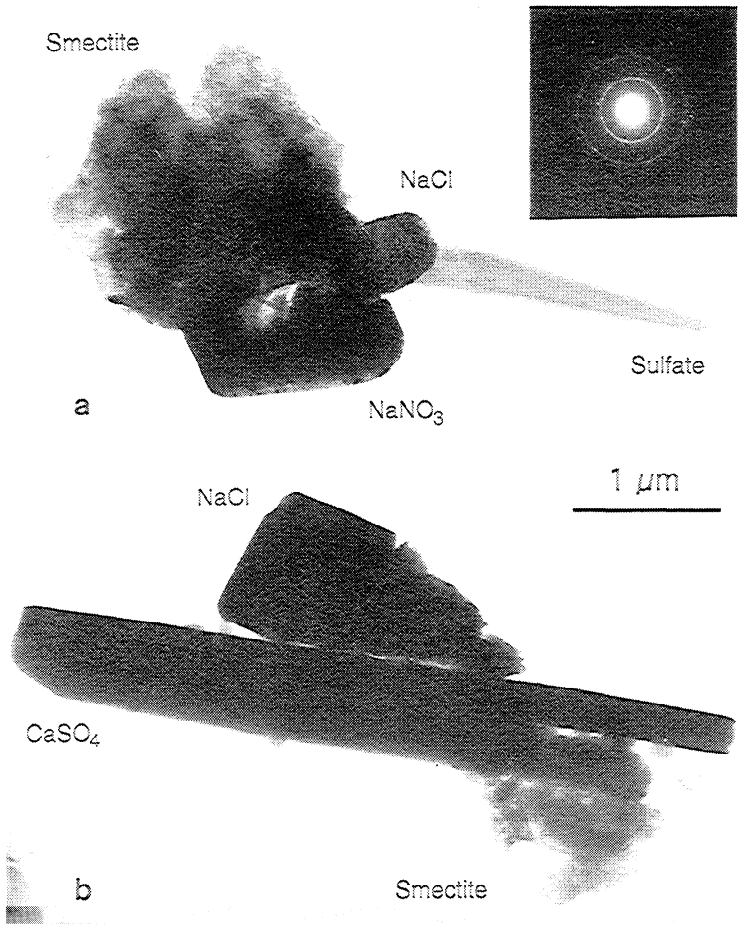

Figure 7. Particles containing minerals of crustal origin. The inserted SAED pattern was obtained from the smectite in Figure 7a (sample 18). The small size of the smectite platelets and their disordered arrangement results in broad, diffuse reflections forming rings. The $CaSO_4$ particle in Figure 7b (sample 19) is anhydrite.

oxidation by O_3 [*Chameides and Stelson,* 1992] on particles in that sample.

A process of sea-salt conversion can be inferred from Figures 10 to 12 and Table 3. The droplets ejected from the sea first undergo a rapid, partial transformation when O_3 oxidizes SO_2 to form mixed-cation sulfate. This mechanism and reactions with atmospheric N-bearing species produce the particles in group I. Subsequent nitrate formation is possible both night and day if NO_x or HNO_3 are available, producing group II and IV particles. NO_3^- can completely replace Cl^- during the day, most likely by direct reactions between NaCl and HNO_3. The products of this reaction are in group III. Na_2SO_4 (group V) particles form from sea salt when high concentrations of S (probably from anthropogenic sources) undergo O_3 oxidation in the marine boundary layer.

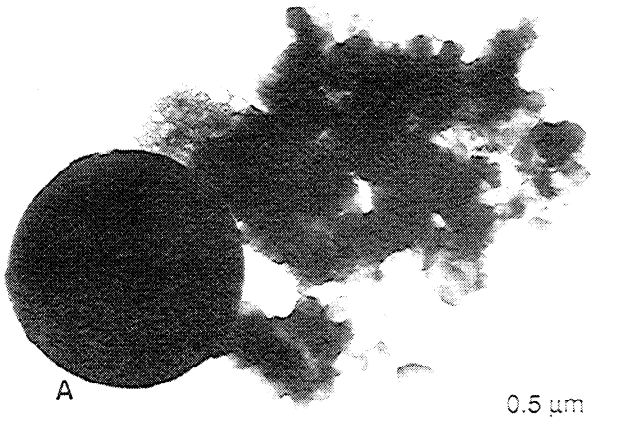

Figure 8. Rounded aluminosilicate (labeled A) with mixed-cation sulfate (sample 19).

Cl Loss

Variable amounts of Cl are lost from particles in groups I to V. As discussed above, this loss is accompanied by sulfate and nitrate formation. *Keene et al.* [1990] reported Cl losses that were not entirely compensated by $SO_4^=$ and NO_3^- in marine aerosols. In addition, *Pszenny et al.* [1993b] described the production of atomic Cl by an unidentified process.

If Cl^- is volatilized from sea-salt particles, the excess Na^+ has to be balanced by other anions. They presumably become available in the same reaction that releases the Cl^-. In our present TEM study we tried to identify all components in the particles. We did not detect any "new" species that could explain "uncompensated" Cl losses, although amorphous substances that contain elements lighter than Na could escape our attention. They could occur in group I, II, and IV particles, many of which contain poorly crystallized phases. *Chameides and Stelson* [1992, 1993] proposed that marine fulvic acids

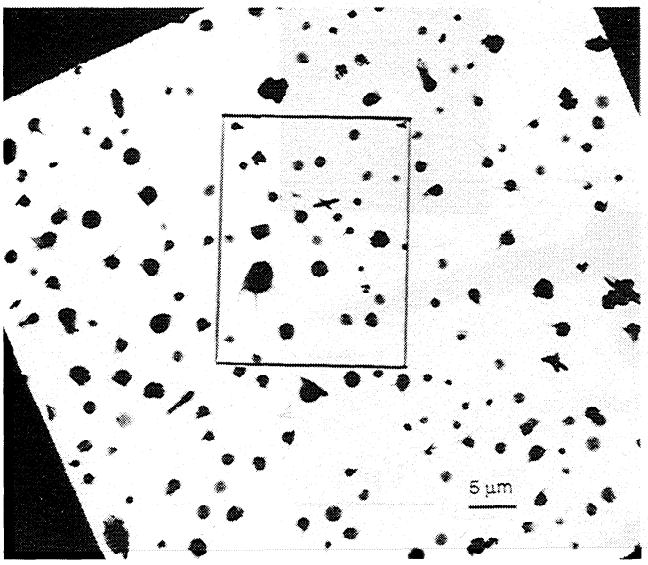

Figure 9. Low-magnification TEM image of a grid mesh in sample 20. EDS spectra were obtained from all particles within the outlined area; their compositions are plotted in Figure 12c.

(MFA) could volatilize Cl from sea salt. We studied EDS spectra from group I, II, and IV particles to assess whether they contain C, which could be an indication of reactions with MFA; however, we found no systematic increases in the C peak. Since we identified all components of group III and V particles as $NaNO_3$ and Na_2SO_4 (Figures 5 and 3, respectively), we believe that in these groups Cl losses are fully compensated by nitrate and sulfate.

Continental Effects

The most abundant dust particles are clay minerals, almost all of which are attached to sea salt or its reaction products. Since clay minerals are hygroscopic, they easily form aggregates with other marine aerosol species. The aggregation most likely takes place in clouds [*Andreae et al.*, 1986]. In the dirty samples, especially sample 18, anhydrite ($CaSO_4$) particles are abundant and represent a direct continental input of sulfate to the marine aerosol.

The continental air masses seem to enhance the conversion of sea salt into sulfate. Anthropogenic S is apparently responsible for the formation of group V Na_2SO_4 particles. In the dirty samples, $(NH_4)_2SO_4$ particles occur in the same size range as sea-salt particles (~1 to 2 μm).

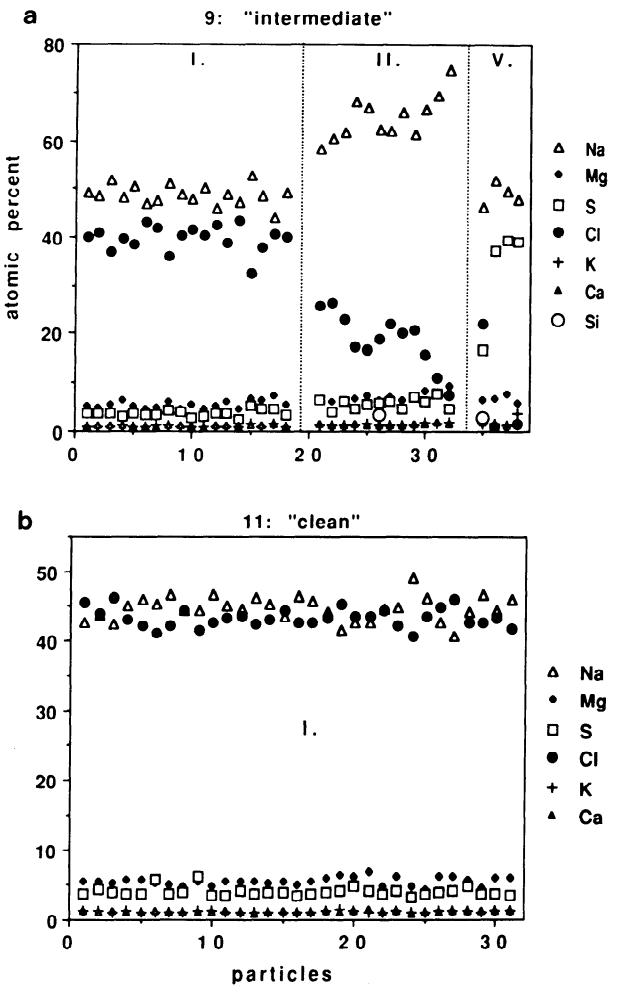

Figure 10. Compositions of particles in (a) sample 9 and (b) sample 11, collected during IL1.

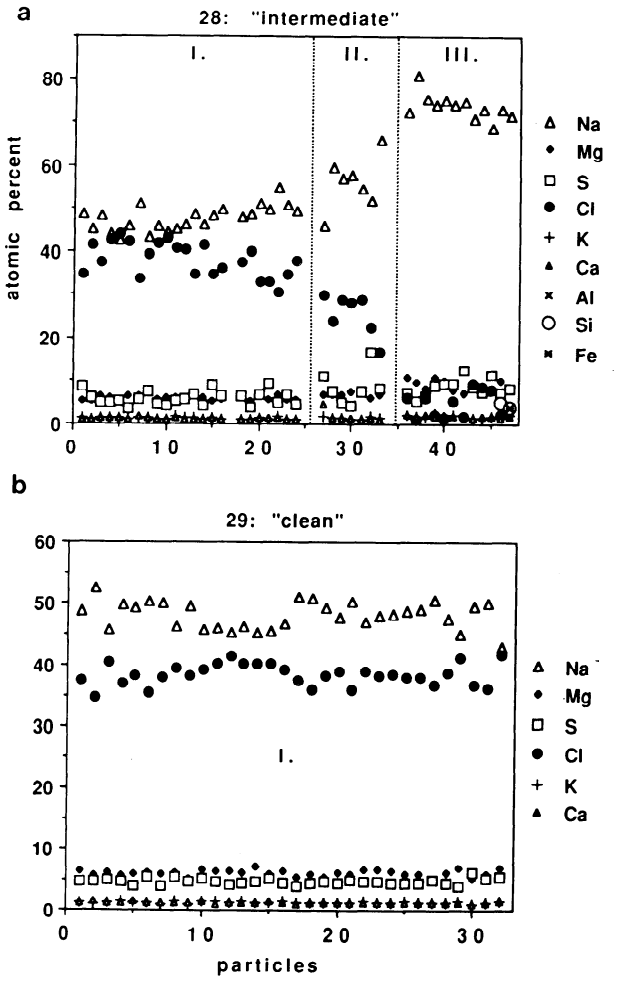

Figure 11. Compositions of particles in (a) sample 28 and (b) sample 29, collected during S1. Two $(NH_4)_2SO_4$ particles and an unidentified particle in sample 28 are not represented in the diagram.

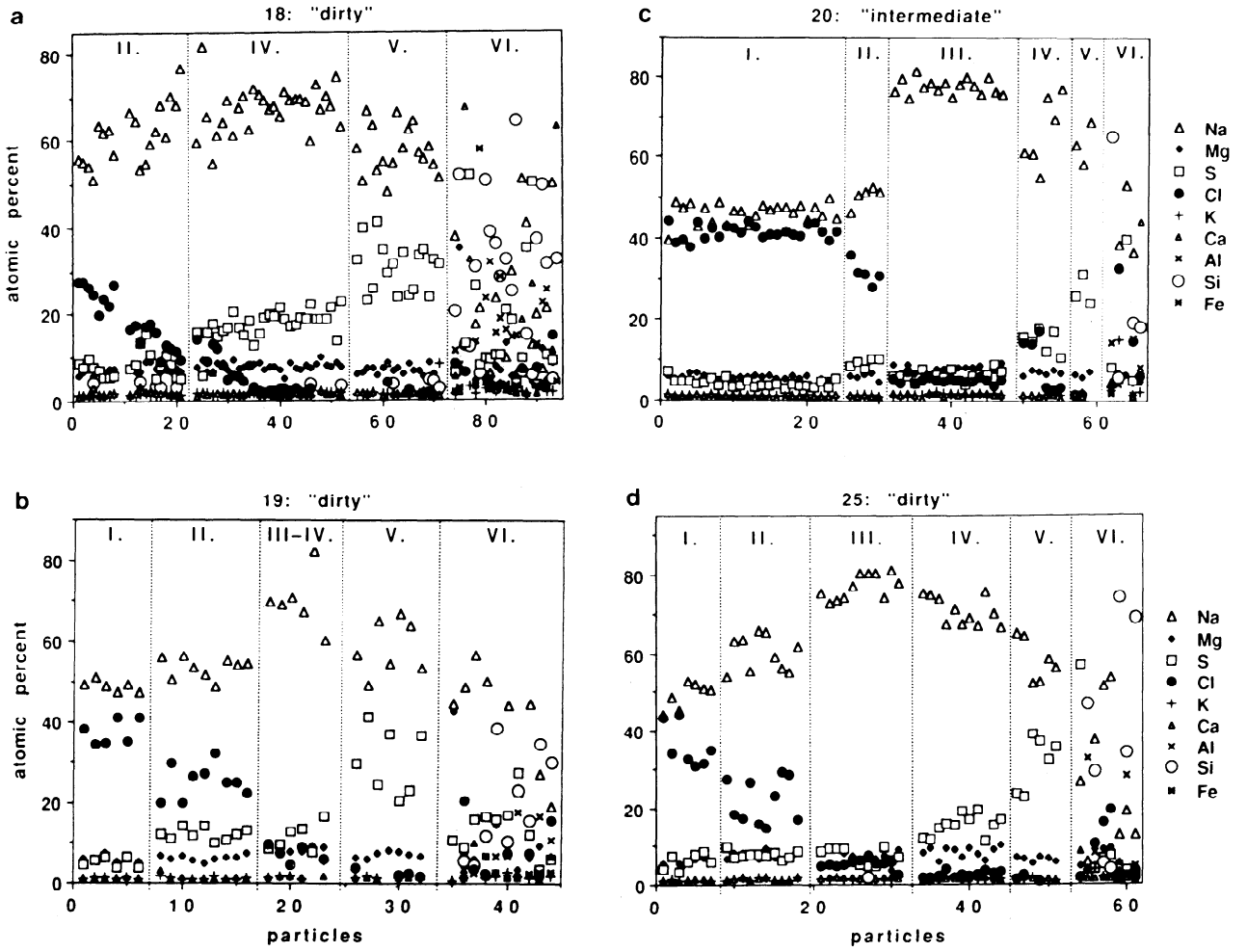

Figure 12. Compositions of particles in (a) samples 18, (b) 19, (c) 20, and (d) 25, collected during IL2. The number of $(NH_4)_2SO_4$ and unidentified particles that are not represented in the diagrams are 6 and 12 in sample 18; 3 and 2 in sample 19; 1 and 1 in sample 20; and 2 and 0 in sample 25, respectively.

Mixing of Aerosol Populations

Particle compositions are uniform in the clean samples, whereas several distinct compositional groups can be distinguished in the dirty samples (Figures 10 to 12). Groups I, III, and V are well defined. Since all particles in groups I to V formed from sea salt, it would be unreasonable to conclude that a particular process acted on a portion of the original sea-salt aerosol particles, while leaving the rest intact. Therefore we think that aerosol populations having different histories are mixed together in some of the intermediate and in all dirty samples.

Group I contains locally produced sea-salt particles, while particles in groups III and V are mixed into the aerosol from other air parcels. It is possible that a part of the conversion of NaCl into $NaNO_3$ and Na_2SO_4 took place in clouds, in which case, particles in groups III and V cycled through clouds, while group I particles did not. The complete conversion to Na_2SO_4 probably resulted from the combined effects of the O_3 oxidation mechanism of *Sievering et al.* [1992, this issue] and

Table 2. Characterization of the Compositional Groups That Were Distinguished in the Eight Samples

Group Number	Major Particle Component	Characterization of Particles
I	NaCl	NaCl with lesser mixed-cation (Na, Mg, K, Ca) sulfates; $NaNO_3$ in some particles
II	"Aged NaCl"	NaCl with mixed-cation sulfates and $NaNO_3$
III	$NaNO_3$	$NaNO_3$ with minor amounts of mixed-cation sulfates
IV	Na_2SO_4 and $NaNO_3$	Na_2SO_4 (with minor Mg, K, Ca) and $NaNO_3$
V	Na_2SO_4	Na_2SO_4 (with minor Mg, K, and Ca)
VI	Silicate	Crustal particles, mainly clay minerals or anhydrite, with various combinations of NaCl, mixed-cation sulfates, and $NaNO_3$

Table 3. Differences Between Atomic Ratios of Na to Mg, K, Ca, S, and Cl Relative to the Values of Seawater

Sample Number	Group Number	Δ Cl/Na	Δ S/Na	Δ A^-/Na	Δ Mg/Na	Δ K/Na	Δ Ca/Na
9	I	-0.34	0.02	0.32	0.01	0.001	0.001
	II	-0.87	0.03	0.83	0	0	0.001
	V	-1.03	0.62	-0.12	0.03	0.005	0.011
11	I	-0.19	0.03	0.16	0.01	0.005	0.005
18	II	-0.86	0.07	0.74	0.01	0.001	0.009
	IV	-1.10	0.20	0.71	0.01	0	0.001
	V	-1.15	0.48	0.23	0.01	0.006	0.008
19	I	-0.39	0.04	0.34	0.02	0.004	0.002
	II	-0.68	0.17	0.37	0.01	0.002	0.004
	III-IV	-1.07	0.11	0.89	0.02	0.006	-0.002
	V	-1.13	0.46	0.24	0.01	0	-0.005
20	I	-0.26	0.03	0.23	0.01	0.002	0.001
	II	-0.54	0.13	0.30	0.01	0.003	0
	III	-1.09	0.02	1.03	–0.01	–0.001	-0.002
	IV	-1.02	0.16	0.68	0	–0.001	-0.003
	V	-1.14	0.37	0.36	–0.01	–0.005	-0.008
25	I	-0.43	0.07	0.34	0.02	0.002	0.003
	II	-0.80	0.07	0.69	0.02	0.003	0.001
	III	-1.09	0.04	0.97	–0.02	–0.002	0
	IV	-1.12	0.16	0.82	0.01	0	-0.001
	V	-1.15	0.49	0.19	0	0.002	0.002
28	I	-0.36	0.06	0.27	0.02	0.005	0.004
	II	-0.71	0.09	0.56	0.01	0.003	0.009
	III	-1.10	0.06	1.01	0.01	0.004	0.002
29	I	-0.36	0.04	0.33	0.02	0.005	0.004
Seawater		Cl/Na= 1.16	S/Na= 0.06	A^-/Na= 0.007	Mg/Na= 0.11	K/Na= 0.022	Ca/Na= 0.022

Ratios are given for compositional groups I to V in each sample as determined from EDS analyses. The column under Δ A^-/Na contains calculated values; A^- stands for anions other than Cl^- and $SO_4^=$ (see text). The ratios for seawater (as listed in the bottom row) are obtained from *Millero and Sohn* [1992].

cycling through clouds. Particles in groups II and IV could have "aged" locally, but they could also have arrived from other air parcels.

When continental air masses are transported to the marine environment, the possibility of mixing of aerosols that have different "chemical ages" increases, as reflected by the heterogeneity of particle compositions in the dirty samples. The results of the mixing of air masses above the Pacific Ocean were observed by *Parrish et al.* [1992] and discussed by *Finlayson-Pitts* [1993] and *Parrish et al.* [1993].

Significant changes occur in the aerosol compositions on a short timescale. On June 13 and June 24 the aerosol changed from intermediate to clean in a matter of hours (samples 9 and 11, and 28 and 29, respectively). On June 19 the aerosol can be characterized by the high sulfate content in the early morning (sample 18), but in the afternoon the dominant Cl^--replacing anion is NO_3^- (sample 20).

Conclusions

Sea-salt-mode aerosol particles were collected above the North Atlantic Ocean. As observed on the TEM grids, most particles are internally mixed, i.e., they consist of combinations of several phases, including NaCl, mixed-cation (Na, Mg, K, Ca) sulfates, $NaNO_3$, Na_2SO_4 (with minor Mg, K, and Ca), $(NH_4)_2SO_4$, and terrestrial minerals (mostly silicates and anhydrite).

Particles of sea-salt origin can be distinguished on the basis of their seawater-like Mg/Na, K/Na, and Ca/Na ratios. The magnitude of the Cl loss from these particles and the amount of sulfate and nitrate that formed on them define distinct compositional groups. Such groups represent different stages during sea-salt conversion, and reflect the effects of reactions between NaCl and atmospheric S- and N-bearing compounds.

In two of the eight samples, particles formed under clean oceanic conditions and have uniform compositions. Their excess sulfate and nitrate probably formed through the oxidation of SO_2 by O_3 in the sea-salt aerosol water and by direct reactions between NO_x (NO_2 and N_2O_5) and NaCl.

Particles that consist mostly of $NaNO_3$ occur in two intermediate and two dirty samples. These samples were collected during the day, when photochemical reactions could result in the formation of HNO_3, which in turn, could volatilize Cl from sea salt and convert NaCl into $NaNO_3$.

The three dirty samples contain many crustal and individual Na_2SO_4 particles. A probable source of this sulfate is anthropogenic SO_2, with sulfate formation taking place either in the aerosol water or in clouds.

Rapid temporal variations in aerosol compositions and the presence of distinct compositional groups indicate that the mixing of aerosol populations having different chemical ages, and some having different sources, played an important role in the formation of aerosol particles that were collected during ASTEX/MAGE.

Appendix

Analytical transmission electron microscopy has so far only been used in a few studies of marine aerosols. Therefore a brief review on the quality of our data is warranted.

EDS analyses of sea-salt particles were performed by *Mouri et al.* [1993], who obtained constant Cl/Na ratios, whereas Mg/Na, K/Na, and Ca/Na correlated with S/Na. However, *Mouri et al.* [1993] assumed that sea-salt particles are internally homogeneous, and they positioned the electron beam at the centers of the particles. By using this method, some components of the particles may have been excluded from the beam; consequently, their compositions may not be representative of the whole particles. *McInnes et al.* [1994] analyzed entire particles and observed Cl depletion and S enrichment in sea-salt particles, as do we.

There is always a risk that the original particles may have transformed in the vacuum of the TEM or under the electron beam. In order to assess such changes, we first looked at the samples with an optical microscope to observe the distribution and approximate sizes of the particles on the grids and to note prominent morphological features such as the long sulfate rods. Then low-magnification TEM images were taken from the same sample regions. There were no apparent differences in the numbers or morphologies of the particles as determined with the two methods. Some samples were studied with the TEM several times during a 1-year period. In a selected area, we analyzed the same particles after 4 months to check the consistency of the X ray analyses; the results were essentially identical.

The shipboard ion chromatography analyses serve as an independent control of our results from the two clean samples that contain particles with uniform compositions. (In the other samples, we could determine the average compositions of groups, but not of the bulk samples.) The mole ratios of Cl^-/Na^+ and non-sea-salt (nss) $SO_4^=/Na^+$ are available from the shipboard measurements for the 1- to 3-μm aerosol fraction. In samples 11 and 29, Cl/Na^+ is 1.03 and 0.89, and nss-$SO_4^=/Na^+$ is 0.027 and 0.044, respectively [*Pszenny,* 1993]. We obtain similar results from our EDS analyses: Cl/Na=0.97 and 0.80, and nss-S/Na=0.03 and 0.04 in samples 11 and 29, respectively.

The above arguments support the notion that changes in particle compositions were negligible during storage and TEM investigations of our samples. However, it is difficult to estimate the extent of changes that the particles suffered during collection. Particles may still react with atmospheric gases while water evaporates from them. However, we expect that these reactions would never produce compositional groups that are as distinct as we observed in several samples. We assume that our results reflect basic compositional distributions of the original airborne particles.

Most of the individual species in the particles are crystalline. Since the reflective properties of aerosol species may depend on whether they are solid or liquid, it is of interest to know when crystallization occurred. *Tang and Munkelwitz* [1993] studied the deliquescence properties of some inorganic aerosols. Applying their results to the Azores samples, we find that many species, particularly Na_2SO_4 and $(NH_4)_2SO_4$, could have been crystalline even in the atmosphere. Three of our samples (25, 28, 29) were collected at such low relative humidities (Table 1) that even NaCl could form crystals while in the air. The morphology of the particle in Figure 5 is characteristic of group III particles in sample 20. This sample was collected at 20.2°C and 79% relative humidity, which is below the deliquescence point of Na_2SO_4, but above that of $NaNO_3$. We think that the sulfate rod in that particle formed in the atmosphere, whereas the major species of the particle, $NaNO_3$, crystallized on the grid.

Acknowledgments. This research was supported by NSF grant ATM-9007796. We thank T. Jensen-Leute and C. Nagamoto for their assistance with aerosol sampling. This research was also supported by a grant (to PRB) from the Atmospheric Chemistry Division of the NSF (ATM-9408704). Electron microscopy was performed at Arizona State University.

References

Andreae, M. O., R. J. Charlson, F. Bruynseels, H. Storms, R. Van Grieken, and W. Maenhaut, Internal mixture of sea salt, silicates, and excess sulfate in marine aerosols, *Science, 232,* 1620-1623, 1986.

Behnke, W., and C. Zetzsch, Heterogeneous photochemical formation of Cl atoms from NaCl aerosol, NO_x and ozone, *J. Aerosol Sci., 21, suppl. 1,* S229-S232, 1990.

Chameides, W. L., and A. W. Stelson, Aqueous-phase chemical processes in deliquescent sea-salt aerosols: a mechanism that couples the atmospheric cycles of S and sea salt, *J. Geophys. Res., 97,* 20,565-20,580, 1992.

Chameides, W. L., and A. W. Stelson, Reply, *J.Geophys. Res., 98,* 9051-9054, 1993.

Cliff, G., and G. W. Lorimer, The quantitative analysis of thin specimens, *J. Microsc., 102,* 203-207, 1975.

Deer, W. A., R. A. Howie, and J. Zussman, *An Introduction to the Rock-Forming Minerals,* p. 696, Longman, White Plains, N. Y., 1992.

Eysel, W., Crystal chemistry of the system Na_2SO_4-K_2SO_4-K_2CrO_4-Na_2CrO_4 and the glaserite phase, *Am. Mineral., 58,* 736-747, 1973.

Eysel, W., H. H. Höfer, K. L. Keester, and T. Hahn, Crystal chemistry and structure of Na_2SO_4(I) and its solid solutions, *Acta Crystallogr., B41,* 5-11, 1985.

Finlayson-Pitts, B. J., Reaction of NO_2 with NaCl and atmospheric implications of NOCl formation, *Nature, 306,* 676-677, 1983.

Finlayson-Pitts, B. J., Comment on "Indications of photochemical histories of Pacific air masses from measurements of atmospheric trace species at Point Arena, California" by D. D. Parrish et al., *J. Geophys. Res., 98,* 14,991-14,993, 1993.

Finlayson-Pitts, B. J., M. J. Ezell, and J. N. Pitts Jr., Formation of chemically active chlorine compounds by reactions of atmospheric NaCl particles with gaseous N_2O_5 and $ClONO_2$, *Nature, 337,* 241-244, 1989.

Hegg, D. A., P. V. Hobbs, and L. F. Radke, Measurements of the scavenging of sulfate and nitrate in clouds, *Atmos. Environ., 18,* 1939-1946, 1984.

Huebert, B. J., et al., Measurements of the nitric acid to NO_x ratio in the troposphere, *J.Geophys. Res., 95,* 10,193-10,198, 1990.

Keene, W. C., A. A. P. Pszenny, D. J. Jacob, R. A. Duce, J. N. Galloway, J. J. Schultz-Tokos, H. Sievering, and J. F. Boatman, The geochemical cycling of reactive chlorine through the marine troposphere, *Global Biogeochem. Cycles, 4,* 407-430, 1990.

Keene, W. C., D. J. Jacob, A. A. P. Pszenny, R. A. Duce, J. J. Schultz-Tokos, and J. N. Galloway, Comment on "Aqueous phase chemical processes in deliquescent sea-salt aerosols: a mechanism that couples the atmospheric cycles of S and sea salt" by W. L. Chameides and A. W. Stelson, *J. Geophys. Res., 98,* 9047-9049, 1993.

Kim, Y., H. Sievering, J. Boatman, D. Wellman, and A. Pszenny, Aerosol size distribution and aerosol water content measurements during the Atlantic Stratocumulus Transition Experiment/Marine Aerosol and Gas Exchange, *J. Geophys. Res.*, this issue.

Mamane, Y., and J. Gottlieb, Nitrate formation on sea-salt and mineral particles - a single particle approach, *Atmos. Environ., Part A, 26,* 1763-1769, 1992.

McInnes, L. M., D. S. Covert, P. K. Quinn, and M. S. Germani, Measurements of chloride depletion and sulfur enrichment in individual seasalt particles collected from the marine boundary layer, *J. Geophys. Res., 99,* 8257-8268, 1994.

Millero, F. J., and M. L. Sohn, *Chemical Oceanography,* p. 531, CRC Press, Boca Raton, Fla., 1992.

Mouri, H., K. Okada, and K., Shigehara, Variation of Mg, S, K and Ca contents in individual sea-salt particles, *Tellus, Ser. B, 45,* 80-85, 1993.

Parrish, D. D., C. J. Hahn, E. J. Williams, R. B. Norton, F. C. Fehsenfeld, H. B. Singh, J. D. Shetter, B. W. Gandrud, and B. A. Ridley, Indications of photochemical histories of Pacific air masses from measurements of atmospheric trace species at Point Arena, California, *J. Geophys. Res., 97,* 15,883-15,901, 1992.

Parrish, D. D., C. J. Hahn, E. J. Williams, R. B. Norton, F. C. Fehsenfeld, H. B. Singh, J. D. Shetter, B. W. Gandrud, and B. A. Ridley, Reply, *J. Geophys. Res., 98,* 14,995-14,997, 1993.

Pósfai, M., J. R. Anderson, P. R. Buseck, T. W. Shattuck, and N. W. Tindale, Constituents of a remote Pacific marine aerosol: A TEM study, *Atmos. Environ., 28,* 1747-1756, 1994.

Pszenny, A., The 1992 ASTEX-MAGE data report, Ocean Chem. Div., NOAA Atl. Oceanogr. and Meteorol. Lab., Miami, Fla., 1993.

Pszenny, A., C. Fischer, A. Mendez, M. Zetwo, and C. Brown, Particle size distributions of chloride deficit in the marine boundary layer over the Atlantic and Pacific Oceans (abstract), *Eos Trans., AGU, 74* (43), Fall Meet. Suppl., 127, 1993a.

Pszenny, A., W. C. Keene, D. J. Jacob, S. Fan, J. R. Maben, M. P. Zetwo, M. Springer-Young, and J. N. Galloway, Evidence of inorganic chlorine gases other than hydrogen chloride in marine surface air, *Geophys. Res. Lett., 20,* 699-702, 1993b.

Sethi, V., and W. John, Particle impaction patterns from a circular jet, *Aerosol Sci.Technol., 18,* 1-10, 1993.

Sievering, H., J. Boatman, J. Galloway, W. Keene, Y. Kim, M. Luria, and J. Ray, Heterogeneous sulfur conversion in sea-salt aerosol particles: the role of aerosol water content and size distribution, *Atmos. Environ., Part A, 25,* 1479-1487, 1991.

Sievering, H., J. Boatman, E. Gorman, Y. Kim, L. Anderson, G. Ennis, M. Luria, and S. Pandis, Removal of sulphur from the marine boundary layer by ozone oxidation in sea-salt aerosol, *Nature, 360,* 571-573, 1992.

Sievering, H., E. Gorman, T. Ley, A. Pszenny, M. Springer-Young, J. Boatman, Y. Kim, C. Nagamoto, and D. Wellman, Ozone oxidation of sulfur in sea-salt aerosol particles during the Azores Marine Aerosol and Gas Exchange experiment, *J. Geophys. Res.,* this issue.

Tang, I. N., and H. R. Munkelwitz, Composition and deliquescence properties of hygroscopic aerosols, *Atmos. Environ., Part A, 27,* 467-473, 1993.

J. R. Anderson and P. R. Buseck, Departments of Geology and Chemistry, Arizona State University, Box 87-1404, Tempe, AZ 85287.

M. Pósfai, Department of Mineralogy, University of Veszprem, H-8201 Veszprem, POB 158, Hungary. (e-mail: posfaim@almos.vein.hu)

H. Sievering, Center for Environmental Sciences, University of Colorado - Denver, Box136, Denver, CO 80217.

(Received May 2, 1994; revised April 18, 1995;
accepted April 19, 1995.)